Comparison of Different Iron-oxide Agent Detection Methods using a Single Dataset

G. Varma[1], R. Tavare[1], H. Dahnke[2], S. Keevil[1], and T. Schaeffter[1]

[1]Division of Imaging Sciences, King's College London, London, United Kingdom, [2]Philips Research Laboratories, Hamburg, Germany

Introduction: Detection of super-paramagnetic iron-oxide (SPIO) at varying sensitivities can be achieved through its inherent negative contrast or by positive contrast methods. Over the past few years a number of positive contrast methods have been proposed: 1. A "white marker" [1] is induced by conservation of signal in areas of susceptibility after application of an additional dephasing gradient in the slice direction. 2. Inversion recovery on-resonance (IRON) [2] suppresses signals centred on the water frequency and leaves off-resonant spins available for subsequent imaging. 3. Susceptibility gradient mapping (SGM) [3] determines the shift in *k*-space of local areas within an image. Recently, these methods were compared to detect iron-oxide labelled cells [4]. However in that study all methods were applied to acquire different datasets after optimising each separately, making a direct comparison difficult. In this study we demonstrate all methods can be derived from *one* multi-gradient echo imaging dataset in a post-processing step. This ensures optimal settings for the different methods and allows a direct comparison on the same dataset.

Methods: A 3D dataset is obtained using multi-gradient echo imaging that obtains the complete *k*-space for each echo time (TE). This 4D (3 spatial plus time) dataset allows the production of quantitative R_2* maps as well as negative (T_2*-weighted) and positive contrast (IRON, gradient dephasing, and SGM) images:

- T_2* weighted – images for increasing TEs are taken from the multi-echo gradient readout.
- R_2* map - the images at different echo times (TEs) give a representation of the free induction decay (FID). Applying a least-squares exponential fit to the FID allows a R_2*/T_2* value to be calculated on a pixel-by-pixel basis.
- IRON - the signal is displayed in terms of its frequency components through a Fast Fourier Transform (FFT) of the FID [5]. This spectroscopic imaging data allows the suppression of the frequencies around those relating to water spins on-resonance using different filters (Fig.1a). An optimal setting of the filter is ensured by histogram analysis over all or selected pixels in the spectroscopic imaging data to determine the centre frequency and suppression bandwidth. IRON images, in which signal from off-resonance spins are displayed, can be produced upon application of an inverse FFT.
- Gradient dephasing - the "white marker" technique is achieved post-process by applying a pixel-wise FFT to data along the slice direction. The result represents the spatial frequencies related to a specific pixel and any shift from the centre frequency is thus taken to be the result of incomplete refocusing of the signal for a central projection along the k_z-axis due to the presence of an additional local gradient. Therefore the projections above/below that at the centre correspond to images in which an additional gradient would have been applied to change the location of the echo acquisition in k_z-space.
- SGM - accomplished by again applying 1D FFTs, but to a set of 5 adjacent pixels/slices in all 3 orthogonal directions separately and then combined to provide a susceptibility gradient vector. SGM can be compared to the post-processing method for gradient dephasing and in both cases the shift in *k*-space, $M_i \approx -\left(G_i^{suscep}.TE\right)/\left(G_i^{imaging}.\tau_i\right)$ (1), where τ is the gradient duration and $i = x,y,z$ [3] (i is limited to the *z*-direction for "white marker" method).

The phantom used consists of 4 test-tubes containing solutions of the SPIO Endorem® at successively halved concentrations, located around a control tube of gelatine, all of which are placed in a solution of gelatine (Fig.1b-c). MR scanning is conducted in a Philips 3.0T Achieva scanner, with the phantom inside a quadrature head-coil.

Experimental Results: The multi-gradient echo sequence with 63 echoes, ΔTE~1.2ms, TR=120ms, was utilised to provide a number of T_2*-weighted 256x256 images with 1mm isotropic resolution. Contrast-to-noise (CNR) was used as a sensitivity measure and calculated (Table 1) at an optimal TE for each concentration determined by the R_2* map (Fig.1d). CNR in both T_2* images and the R_2* map consistently showed distinction between the test-tubes, but this was in part due to the relatively homogeneous background of the phantom. IRON images produced in the scanner and post-process (Fig.1e-f) were found to have comparable CNRs (Table 2), but the contrast was dependent upon the filter's position and size. The linear proportionality of a shift in *k*-space with TE (1) resulted in the effect of SPIO's susceptibility gradient becoming more pronounced for gradient dephasing and SGM (Fig.1i-j; Table 1). Therefore the correct choice of TE is important to ensure a sufficient shift in *k*-space. The CNR of gradient dephasing was low and only provided a useful contribution when there was susceptibility in the slice direction (Fig.1g-h; Table 3).

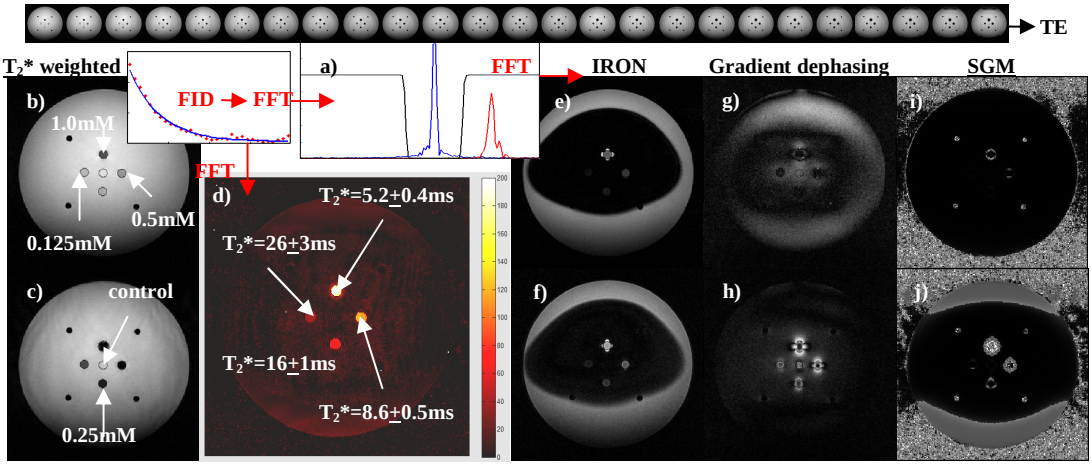

Figure 1. (top) multi-echo images, (a) on-(blue) & off-resonance (red) signal representations with filter (black) for IRON, T_2* images for TEs (b) 4.7ms (c) 25.9ms, (d) R_2* map, IRON images (TE~2ms;BW=100Hz) (e) post-process & (f) from scanner, "white marker" images (TE=16.5ms) at (g) slice 6 (h) slice 12, & SGM for TEs (i) 4.7ms (j) 25.9ms

IRON	*1.0mM*	*0.5mM*	*0.25mM*	*0.1mM*
CNR (e)	34.6	16.4	7.9	4.3
CNR (f)	30.1	17.0	9.1	3.7

Table 2. CNR for IRON MRI (Fig.1f) & post-process (Fig.1e)

White Marker	*1.0mM*	*0.5mM*	*0.25mM*	*0.1mM*
Slice 6	-5.4	-5.8	-6.5	-5.7
Slice 12	8.6	6.0	0.2	0.3

Table 3. CNR for "white marker" images (Fig.1g-h)

T_2 weighted*	*1.0mM*	*0.5mM*	*0.25mM*	*0.125mM*
TE=4.7ms	-35.8	-18.3	-13.6	-10.1
TE=9.4ms	-54.6	-38.5	-26.1	-19.3
TE=16.5ms	-56.6	-52.8	-41.0	-28.8
TE=25.9ms	-49.2	-49.5	-44.2	-32.4
R_2* map	17.4	10.3	5.8	3.5
SGM				
TE=4.7ms	68.5	36.9	7.2	3.5
TE=9.4ms	180	77.1	18.5	3.9
TE=16.5ms	387	147	57.2	4.8
TE=25.9ms	433	165	58.6	15.4

Table 1. CNR of T_2*-weighted images, R_2*-map and SGM images

Conclusions: The CNR provided by R_2* mapping plus the quantitative information gives it the edge. However if time for data acquisition is not available, T_2* imaging gives a high CNR, but requires different TEs for different concentrations. The high sensitivity of SGM and T_2* imaging suggests a combination of these two methods is ideal. Data acquired for T_2* images and SGM at 2 different TEs to address different concentrations would provide a more sensitive differentiation to the background. Future work would concentrate on application of the above methods to datasets involving SPIO labelled cells for comparisons to be made in preparation for *in-vivo* tracking.

References: [1] Seppenwoolde et al. MRM 50:784-790 (2003), [2] Stuber et al. Proc. ISMRM 13:2608 (2005), [3] Dahnke et al. Proc. ISMRM 14:361 (2006), [4] Liu et al. Proc. ISMRM 15:3453(2007), [5] Mansfield et al. MRM 1:370-386 (1984)